Aalborg Universitet

Risk-Involved Optimal Operating Strategy of a Hybrid Power Generation Company: A Mixed Interval-CVaR Model

Khaloie, Hooman; Anvari-Moghaddam, Amjad; Contreras, Javier; Siano, Pierluigi

Risk-Involved Optimal Operating Strategy of a Hybrid Power Generation Company: A Mixed Interval-CVaR Model

Hooman Khaloie[1], Amjad Anvari-Moghaddam[2], Javier Contreras[3], Pierluigi Siano[4]

(1) Iran's National Elites Foundation, Kerman Regional Electric Company, Kerman, Iran

(2) Department of Energy Technology, Aalborg University, 9220 Aalborg East, Denmark

(3) Escuela Técnica Superior de Ingenieros Industriales, University of Castilla–La Mancha, Ciudad Real 13071, Spain

(4) Department of Management & Innovation Systems, University of Salerno, Fisciano, Italy

Corresponding Author: Hooman Khaloie, Email: hoomankhaloiee@gmail.com

---

Abstract

In this paper, a hybrid power generation company consisting of a concentrated solar power unit, wind turbines, a battery system, and a demand response provider is established to take part in electricity markets. The operating strategy of the hybrid power generation company in day-ahead and adjustment (intraday) markets is determined based on their coordinated operation. To tackle the intrinsic uncertainties, for the first time, a mixed stochastic-interval model is proposed which addresses the uncertainty in demand response and solar energy via interval optimization. The examined problem is formulated as a multi-objective optimization problem in which the risk of both stochastic and interval parameters can be involved. On this basis, the proposed operating strategy covers three objective functions, namely, expected radius and midpoint of the hybrid power generation company's profit together with the conditional value-at-risk. Accordingly, the normal boundary intersection and lexicographic optimization techniques are utilized to derive feasible solutions. Lastly, numerical results are presented and the performance of the proposed framework is

investigated. The results indicate that the suggested model can be efficiently used to handle the decision-maker's preference over interval and stochastic parameters, and the risk criterion associated with interval parameters becomes larger as the forecasting errors increase.

1. Introduction

The interest in renewable sources is becoming increasingly prominent globally. Among various renewable sources, the most prominent growth across the world is related to solar and wind energy [1]. However, running a 100% renewable electricity network without exploiting large-scale hydroelectric units and energy storage facilities is not feasible on account of the intermittency of solar and wind energy [2]. In this regard, harnessing the intermittent output power of renewable energy sources has been known as one of the most significant factors in the utilization of energy storage systems in electricity industries.

Concerning solar energy, two distinct technologies, namely, photovoltaic and Concentrated Solar Power (CSP), can be exploited for electricity generation [3]. Aside from lower financial and investment risks of photovoltaic technology, 24-hour electricity generation is the most promising advantage of CSP technologies over photovoltaic units [4]. Simply put, overcoming the intermittency of solar energy is the most prominent factor for governments and generation companies to move towards CSP technologies. Spain and the United States are the leaders of electricity generation by CSP technologies worldwide [5], while China ranked first in the photovoltaic generation [4]. Following the increasing interest in CSP technologies, the evaluation and examination of CSP units in numerous power system studies have been one of the research priorities across the world. Du *et al.* did two detailed studies on the role of the CSP units in short-term [6] and long-term power system operations [7]. In [6], the unit commitment problem in the presence of CSP units has been developed, while the generation and

transmission expansion problem with CSP units has been discussed in [7]. Xu and Zhang [8] addressed the joint look-ahead economic dispatch and Day-Ahead (DA) unit commitment issue with CSP and wind resources. They found that wind and CSP resources offer considerable advantages to decrease operational costs.

From another perspective, the participation problem of CSP resources in electricity markets has been another recent research interest [9]-[13]. As one of the first studies within this context, Dominguez *et al.* [9] provided a short-term trading model for a CSP unit in the DA market. The model proposed in [9] has been developed based on a stochastic-robust framework. Zhao *et al.* [10] established an Information Gap Decision Theory (IGDT)-based optimization structure for the optimal behavior of a CSP-demand response system in the DA market, while both uncertainties arising from market and CSP were modeled using IGDT method. He *et al.* [11] extended the model proposed in [9] for joint DA, reserve, and regulation markets, while the uncertainty appraisal technique was similar to [9]. Yu *et al.* [12] employed the downside risk approach to address the offering strategy of a CSP system in the DA market. Wu *et al.* [13] proposed a profit-sharing architecture for a hybrid wind-CSP system using a two-stage stochastic programming model. Fang and Zhao [14] developed a look-ahead offering model for a CSP system along with wind turbines using chance-constrained programming.

A broad domain of published works within the context of offering and bidding problems arises from multifarious uncertainty appraisal techniques, electricity market structures, systems under study, and target markets. Accordingly, Zhao *et al.* [15] focused on the DA bidding and offering strategy of electric vehicle aggregators by means of information gap decision theory. Moiseeva and Hesamzadeh [16] suggested a modified Benders technique for addressing the bidding strategy of a hydropower producer, whereas the uncertain sources were handled with stochastic scenarios. By centering on pay-as bid markets, Mazzi *et al.* [17] established a two-stage linear offering framework in DA and real-time markets for thermal units. Shafiee *et al.* [18] utilized robust optimization to

3

derive offering and bidding curves of a price-maker storage facility in the DA market. In [19], Naziri Moghaddam *et al.* assessed the joint sizing and operation problem of a battery facility along with wind turbines. AlAshery *et al.* [20] examined the application of second-order stochastic dominance on the optimal offering strategy of a wind farm in the DA energy market. A two-stage data-driven risk-constrained operating strategy for combined-cycle units was proposed in [21], concentrating on the real-time market. Hasankhani *et al.* [22] and Koltsaklis *et al.* [23] proposed a stochastic and deterministic scheduling models for microgrids. Moreover, Fazlalipour *et al.* [24] and Çavuş *et al.* [25] utilized Conditional Value-at-risk (CVaR) to address risk in stochastic programming models. Khaloie *et al.* in [26] and [27] developed robust and probabilistic-possibilistic models for the self-scheduling problem of different energy entities. Xu *et al.* [28] established a distributionally robust optimization model for the self-scheduling of a wind-battery system in the DA electricity market. Faraji *et al.* in [29] and [30] suggested various enhanced forecasting models based on artificial neural networks to better capture uncertainties in self-scheduling problems.

In the literature reviewed above, the following research shortcomings or unaddressed issues are found:

1. The operating strategy for a market agent having wind turbines, CPS unit, a battery system, and a Demand Response Provider (DRP) have not been formulated yet.

2. Yet, no optimization has been conducted to accommodate the uncertainty of DRP's load via interval optimization. Accordingly, there is no related work in the literature that addresses both DRP's load and thermal power of the CSP's solar field simultaneously via interval optimization.

3. Concerning both stochastic and interval uncertain sources, no work exists in the literature that models the financial risks emanating from multiple stochastic and interval parameters.

Based on the above unaddressed issues, this paper establishes a Mixed

4

Stochastic-Interval (MSI) model for the operating strategy of a CSP unit, a battery system, wind turbines, and a DRP in the DA and adjustment markets. A multi-stage scenario-based model is employed to reflect the uncertain nature of market parameters and wind generation. In contrast, the interval optimization is exploited as a remedy to the lack of adequate historical data to capture the uncertainties emanating from DRP's load and thermal power of the CSP's solar field with probability density functions. The proposed MSI methodology is formulated as a multi-objective linear programming problem in which the Normal Boundary Intersection (NBI) and lexicographic optimization techniques are employed to find Pareto optimal points. The main contributions of this paper with respect to previous works, can be listed as follows:

1. For the first time in literature, an integrated operating strategy in the DA and adjustment markets is proposed and formulated for a Hybrid Power Generation Company (HPGC) considering the coordinated interactions among wind turbines, a CSP unit, a battery system, and a DRP.

2. Uncertainties stemming from DRP's load and the thermal power of the CSP's solar field are simultaneously modeled by means of interval numbers. In this regard, interval optimization merely requires the confidence interval of uncertain parameters, without essentially being aware of the exact probability density function of uncertainties. Besides, a better insight will be gained to the decision-making process by obtaining the optimal interval of output variables via employing this method.

3. An innovative risk-involved MSI methodology is constructed that enables the HPGC to concurrently evaluate the financial risks faced by the HPGC, emanating from multiple interval and stochastic uncertain sources. The proposed MSI methodology in this paper differs from the approach suggested in [31]. In [31], the risk of stochastic parameters is not controlled, and besides, the MSI architecture was formulated as a single-objective optimization approach.

This paper is organized as follows: Assumptions, methods, and materials are

5

presented in Section 2. Case studies are detailed in Section 3, and Section 4 summarizes the conclusions.

2. Assumptions, Methods, and Materials

As a first step, this section describes the model assumptions, and secondly, our proposed model for the considered HPGC is developed. Underlying assumptions include:

1. The HPGC is a price-taker agent, meaning that its operating strategy does not affect market outcomes.

2. The HPGC presents offering and bidding powers to the DA and adjustment markets while only coping with its over- and under-generation energy deviations in the real-time market.

3. The historical data on market prices and wind generation is available for the HPGC. Therefore, stochastic scenarios [32] under a three-stage model account for the uncertainty of the above parameters, as shown in Fig. 1. Any stage of the considered three-stage model signifies a spot in time in which the HPGC makes a specific decision. From the viewpoint of the HPGC, the volume of attainable data varies from one stage to another one.

4. The HPGC does not have access to enough historical data on DRP's load and thermal power of the CSP's solar field. Hence, we introduce the uncertainty of the these parameters through interval numbers.

As we argued above, the uncertainty of market prices and wind generation are addressed by scenarios, and the uncertainty of DRP's load and thermal power of the CSP's solar field is covered through interval numbers [33]. To hedge against the risk of both stochastic scenarios and interval numbers, a new methodology is adopted in this paper. In the proposed methodology, the radius of the HPGC profit and CVaR are the risk criteria corresponding to interval numbers and stochastic scenarios, respectively. The procedure of the elaborated risk-based MSI architecture embraces the following steps:
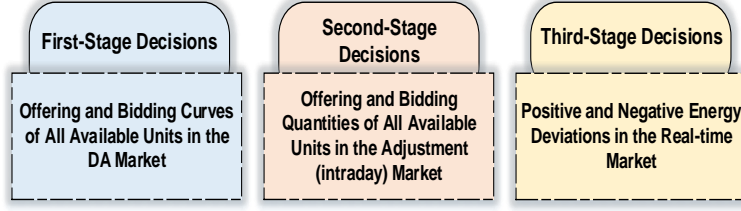
6

Figure 1: The overview of the proposed three-stage decision-making model.

1. Collect all stochastic scenarios and interval numbers associated with the uncertainty origins.

2. Formulate the objective function and technical constraints of the HPGC based on stochastic programming while treating interval numbers as deterministic parameters. The HPGC is seeking to maximize its daily profit (€), which mathematically is equal to the sum of the obtained profits by each member of the HPGC as follows:

$$\text{Max } F^{\text{Sys}} = \sum_{s=1}^{N_S} \pi_s [\text{Profit}_s^C + \text{Profit}_s^W + \text{Profit}_s^B + \text{Profit}_s^{DR}] \qquad (1)$$

where Profit_s^C, Profit_s^W, Profit_s^B, Profit_s^{DR} are profit (€) per scenario for the CSP system, wind turbines, battery system, and DRP, respectively, and π_s refers to the probability of each scenario. The operating profit of the CSP system is equivalent to its total earning made by participation in the DA and adjustment markets, as expressed in (2).

$$\text{Profit}_s^C = \sum_{t=1}^{N_T} \varrho_{t,s}^D \xi_{t,s}^{D,C} q_t + \varrho_{t,s}^A \xi_{t,s}^{A,C} q_t \quad \forall s \qquad (2)$$

where $\varrho_{t,s}^D$ and $\varrho_{t,s}^A$ denote the DA and adjustment market prices, respectively, $\xi_{t,s}^{D,C}$ and $\xi_{t,s}^{A,C}$ are related to the corresponding offering powers of the CSP system in the DA and adjustment markets, respectively, and q_t is time period duration which is set to one hour in this paper. The second profit term of (1), i.e., the gained profit by wind turbines, is presented in (3). The positive terms of the first row state the income from submitting

offering powers in the DA and adjustment markets, while the negative term represents the expenses due to energy procurement in the adjustment market. The second row of (3) addresses the income and expense terms of the wind turbines in the real-time market, resulting from energy deviations.

$$\text{Profit}_s^W = \sum_{t=1}^{N_T} \varrho_{t,s}^D \xi_{t,s}^{D,W} q_t + \varrho_{t,s}^A \xi_{t,s}^{A,W,se} q_t - \varrho_{t,s}^A \xi_{t,s}^{A,W,bu} q_t$$
$$+ \left(\varrho_{t,s}^D \iota_{t,s}^+ \Lambda_{t,s}^+ \right) - \left(\varrho_{t,s}^D \iota_{t,s}^- \Lambda_{t,s}^- \right) \quad \forall s \tag{3}$$

where $\xi_{t,s}^{D,W}$ and $\xi_{t,s}^{A,W,se}$ represent the offering powers of the wind turbines in the DA and adjustment markets, whereas $\xi_{t,s}^{A,W,bu}$ refers to their bidding power in the adjustment market. $\iota_{t,s}^+$ and $\iota_{t,s}^-$ stand for over- and under-generation imbalance price ratios, while $\Lambda_{t,s}^+$ and $\Lambda_{t,s}^-$ are corresponding over- and under-generation energy deviations in the real-time market. The earned profit by the battery system is formulated in (4). The positive terms of (4) are related to the battery's income through submitting offering powers in the DA and adjustment markets. In contrast, the negative terms denote the battery's expenses owing to submitting the bidding powers in the aforementioned markets.

$$\text{Profit}_s^B = \sum_{t=1}^{N_T} \varrho_{t,s}^D \xi_{t,s}^{D,B,dis} q_t - \varrho_{t,s}^D \xi_{t,s}^{D,B,ch} q_t + \varrho_{t,s}^A \xi_{t,s}^{A,B,dis} q_t - \varrho_{t,s}^A \xi_{t,s}^{A,B,ch} q_t$$
$$\forall s \tag{4}$$

where $\xi_{t,s}^{D,B,dis}$ and $\xi_{t,s}^{A,B,dis}$ are battery's offering powers in the DA and adjustment markets, while $\xi_{t,s}^{D,B,ch}$ and $\xi_{t,s}^{A,B,ch}$ stand for corresponding bidding powers. The last term of (1), namely, the profit arising from DRP's operating strategy, is presented in (5). The first term of (5) denotes the DRP's income from the DA market, while the next term appertains to its revenue from the adjustment market. The third term is the DRP's incentive owing to its participation in the DA and adjustment markets, whereas the last term denotes the received income of the DRP resulting

from the elastic demand. It has to be noted that a fixed incentive rate scheme is taken into account to model the incentive.

$$\text{Profit}_s^{\text{DR}} = \sum_{t=1}^{N_T} \varrho_{t,s}^D \varpi_{t,s}^D q_t + \varrho_{t,s}^A \varpi_{t,s}^A q_t + \varrho^* \left(\varpi_{t,s}^D + \varpi_{t,s}^A \right) q_t$$

$$+ \frac{1}{2\varphi L_{0,t}} \sum_{b=1}^{N_B} S_b \varpi_{b,t,s}^{\text{Tot\_b}} \quad \forall s \tag{5}$$

where $\varpi_{t,s}^D$ and $\varpi_{t,s}^A$ are the load shedding offer of the DRP in the DA and adjustment markets. ϱ^* stands for the rate of the incentive payment and $\varpi_{b,t,s}^{\text{Tot\_b}}$ refers to the final planned load shedding offer in each piecewise linearized block, while S_b represents blocks' slope. It is noteworthy to say that the basic quadratic model is linearized with a discrete set of piecewise blocks to maintain the linear essence of the mathematical programming problem [34]. Finally, φ is a constant factor linking load and price, and $L_{0,t}$ defines the DRP's load prior to the load shedding. The constraints of the (1) are given in the following subitems.

(a) Technical constraints of the CSP system [9]: Constraint (6) expresses the submitted energy of the CSP system in the DA and adjustment markets, emanating from the power produced by the thermal storage system $\xi_{t,s}^{D/A,\text{SE}}$ and the solar field $\xi_{t,s}^{D/A,\text{FE}}$. Constraint (7) describes the final planned energy of the CSP system $\xi_{t,s}^{\text{Tot,C}}$, the thermal storage system $\xi_{t,s}^{\text{Tot,SE}}$, and the solar field $\xi_{t,s}^{\text{Tot,FE}}$. The electric power output by the thermal storage and the solar field are denoted in (8) and (9), respectively, calculated by multiplying their corresponding thermal powers ($\varsigma_{t,s}^{\text{SE}}$ and $\varsigma_{t,s}^{\text{FE}}$) and conversion efficiencies (β_3 and β_1). Constraints (10) and (11) enforce the ramp-up and ramp-down constraints of the thermal storage, respectively. Note in (10) and (11), $\varsigma_{t,s}^{\text{FS}}$ and β_2 are the conveyed thermal power from the solar field to the thermal storage and its corresponding efficiency, respectively, while RUR^{ch} and RDR^{dis} represent ramp-up and ramp-down bounds of the thermal storage system during charging and discharging, respectively. To bind the maximum limit of the whole exploited thermal

energy in the solar field, constraint (12) is imposed, where $\mathrm{EF_t}$ is the forecasted output thermal power of the solar field. This constraint enforces that the overall thermal power transferred from the solar field to the power block and thermal storage should be lower than the forecasted output thermal power of the solar field. To keep the whole exploited thermal power for generating electricity within its permissible upper and lower boundaries, constraint (13) is enforced. In other words, constraint (13) limits the transferred thermal power to the powerblock. It is worth noting that x_t is a binary variable reflecting the commitment state of the CSP system. The stored energy update function of the storage system $\varsigma_{t,s}^S$ is captured via (14) and (15). In fact, these constraints calculate the amount of available thermal energy in the thermal storage. Constraint (16) guarantees to maintain this variable inside its technical maximum and minimum values ($\varsigma^{S,Max}$ and $\varsigma^{S,Min}$). To save space, the limits pertaining to minimum down and up times of the CSP system are not given here, while they can be found in [32].

$$
\begin{bmatrix} \xi_{t,s}^{D,C} \\ \xi_{t,s}^{A,C} \end{bmatrix} = \begin{bmatrix} \xi_{t,s}^{D,SE} \\ \xi_{t,s}^{A,SE} \end{bmatrix} + \begin{bmatrix} \xi_{t,s}^{D,FE} \\ \xi_{t,s}^{A,FE} \end{bmatrix} \quad \forall t, \forall s \tag{6}
$$

$$
\begin{bmatrix} \xi_{t,s}^{Tot,C} \\ \xi_{t,s}^{Tot,SE} \\ \xi_{t,s}^{Tot,FE} \end{bmatrix} = \begin{bmatrix} \xi_{t,s}^{D,C} \\ \xi_{t,s}^{D,SE} \\ \xi_{t,s}^{D,FE} \end{bmatrix} + \begin{bmatrix} \xi_{t,s}^{A,C} \\ \xi_{t,s}^{A,SE} \\ \xi_{t,s}^{A,FE} \end{bmatrix} \quad \forall t, \forall s \tag{7}
$$

$$
\xi_{t,s}^{Tot,SE} = \beta_3 \varsigma_{t,s}^{SE} \quad \forall t, \forall s \tag{8}
$$

$$
\xi_{t,s}^{Tot,FE} = \beta_1 \varsigma_{t,s}^{FE} \quad \forall t, \forall s \tag{9}
$$

$$
\beta_2 \left(\varsigma_{t+1,s}^{FS} - \varsigma_{t,s}^{FS} \right) \leq \mathrm{RUR}^{ch} \quad \forall t = 0, \ldots, N_T - 1, \forall s \tag{10}
$$

10

$$\xi_{t,s}^{Tot,SE} - \xi_{t+1,s}^{Tot,SE} \leq RDR^{dis} \quad \forall t = 0, \ldots, N_T - 1, \forall s \qquad (11)$$

$$\varsigma_{t,s}^{FE} + \varsigma_{t,s}^{FS} \leq EF_t \quad \forall t, \forall s \qquad (12)$$

$$\varsigma^{E,Min} x_t \leq \varsigma_{t,s}^{FE} + \varsigma_{t,s}^{SE} \leq \varsigma^{E,Max} x_t \quad \forall t, \forall s \qquad (13)$$

$$\varsigma_{t,s}^{S} = \varsigma_0 + \beta_2 \varsigma_{t,s}^{FS} - \varsigma_{t,s}^{SE} \quad \forall t = 1, \forall s \qquad (14)$$

$$\varsigma_{t,s}^{S} = \varsigma_{t-1,s}^{S} + \beta_2 \varsigma_{t,s}^{FS} - \varsigma_{t,s}^{SE} \quad \forall t \geq 2, \forall s \qquad (15)$$

$$\varsigma^{S,Min} \leq \varsigma_{t,s}^{S} \leq \varsigma^{S,Max} \quad \forall t, \forall s \qquad (16)$$

(b) Technical constraints of the battery system [35]: Constraint (17) states the final planned energy of the battery system in any commitment state. Constraint (18) is fulfilled to prevent concurrent discharging and charging of the battery system at a given hour. The volume of the stored energy in the battery system at each period $\varkappa_{t,s}^{B}$ is updated by (19), and hence, constraint (20) holds this value inside the permitted limit.

$$\begin{bmatrix} \xi_{t,s}^{Tot,B,dis} \\ \xi_{t,s}^{Tot,B,ch} \end{bmatrix} = \begin{bmatrix} \xi_{t,s}^{D,B,dis} \\ \xi_{t,s}^{D,B,ch} \end{bmatrix} + \begin{bmatrix} \xi_{t,s}^{A,B,dis} \\ \xi_{t,s}^{A,B,ch} \end{bmatrix} \quad \forall t, \forall s \qquad (17)$$

$$z_t^{dis} + z_t^{ch} \leq 1, \quad \forall t \qquad (18)$$

$$\varkappa_{t,s}^{B} = \varkappa_{t-1,s}^{B} - \left(\frac{1}{\varepsilon^{B,dis}}\right) \xi_{t,s}^{Tot,B,dis} + \varepsilon^{B,ch} \xi_{t,s}^{Tot,B,ch} \quad \forall t, \forall s \qquad (19)$$

$$0 \leq \varkappa_{t,s}^{B} \leq \varkappa^{B,Max}, \quad \forall t, \forall s \qquad (20)$$

where $\xi_{t,s}^{Tot,B,dis}$ and $\xi_{t,s}^{Tot,B,ch}$ represent the battery's final planned energy under discharging and charging states. Binary variables z_t^{dis}

and z_t^{ch} denote the battery's running state, i.e., discharging ($z_t^{dis} = 1$) and charging ($z_t^{ch} = 1$). $\varepsilon^{B,dis}$ and $\varepsilon^{B,ch}$ stand for discharging and charging efficiencies of the battery system, and $\varkappa^{B,Max}$ is the upper boundary of the stored energy in the battery.

(c) Technical constraints of wind turbines and DRP [34],[36]: The sum of the selling powers in the DA and adjustment markets minus the purchasing powers in the adjustment market specifies the final planned energy of wind turbines $\xi_{t,s}^{Tot,W}$, as formulated in (21). Likewise, the final planned load shedding of the DRP $\varpi_{t,s}^{Tot}$ is stated in (22) and (23). Constraint (24) imposes boundaries on the final planned load shedding offers in the time frame, while ρ determines the extent of the load shedding offers that can be submitted by the DRP in the designated markets within the time frame. Recently, blockchain technology has been defined as a new alternative to enhance the participation of DRPs in all sectors of power systems, especially in energy trading [37]. This technology determines predefined parameter of the DRP smartly. However, in this paper, we consider fixed values for predefined parameters pertaining to the participation of DRP in the energy markets.

$$\xi_{t,s}^{Tot,W} = \xi_{t,s}^{D,W} + \xi_{t,s}^{A,W,se} - \xi_{t,s}^{A,W,bu}, \quad \forall t, \forall s \tag{21}$$

$$\varpi_{t,s}^{Tot} = \varpi_{t,s}^{D} + \varpi_{t,s}^{A} \quad \forall t, \forall s \tag{22}$$

$$\varpi_{t,s}^{Tot} = \sum_{b=1}^{N_B} \varpi_{b,t,s}^{Tot\_b} \quad \forall t, \forall s \tag{23}$$

$$0 \leq \sum_{t=1}^{N_T} \varpi_{t,s}^{Tot} \leq \rho \sum_{t=1}^{N_T} L_{0,t} \quad \forall t, \forall s \tag{24}$$

(d) Integrated operating strategy constraints: The participation extent of the CSP system, battery, and DRP in the DA market, together

with their final planned energy, must be limited within their technical capacity, as denoted in (25)-(28). Similarly, the submitted power of wind turbines in the DA market is limited employing (29). In constraints (25)-(29), Ca^C and Ca^W refer to the nominal capacity of the CSP system and wind turbines. Meanwhile, $Ca^{B,dis}$ and $Ca^{B,ch}$ indicate the battery's nominal discharging and charging capacities. It has to be noted that λ specifies the extent of the load shedding offer that can be submitted by the DRP in the designated markets in an hour. From the perspective of the HPGC, the final planned energy is defined as presented in (30). The greatest permissible extent for submitting offering $Ca^{A,Sys,se}$ and bidding $Ca^{A,Sys,bu}$ powers in the adjustment market are defined in (31) and (32), while (33) and (34) guarantee the equivalent constraints. Inequality (35) binds the final planned energy of the HPGC to the permissible limits. The overall deviation in the real-time market $\Lambda_{t,s}$ is defined by (36), whereas the next two constraints, namely, (37) and (38), are applied to maintain the under- and over-generation deviations in the real-time market within the acceptable boundaries. Note that $P^W_{t,s}$ stands for the forecasted power of wind turbines.

$$
\begin{bmatrix} 0 \\ 0 \end{bmatrix} \leq \begin{bmatrix} \xi^{D,CS}_{t,s} \\ \xi^{Tot,CS}_{t,s} \end{bmatrix} \leq \begin{bmatrix} Ca^C x_t \\ Ca^C x_t \end{bmatrix} \quad \forall t, \forall s \tag{25}
$$

$$
\begin{bmatrix} 0 \\ 0 \end{bmatrix} \leq \begin{bmatrix} \xi^{D,B,dis}_{t,s} \\ \xi^{D,B,ch}_{t,s} \end{bmatrix} \leq \begin{bmatrix} Ca^{B,dis} z^{dis}_t \\ Ca^{B,ch} z^{ch}_t \end{bmatrix} \quad \forall t, \forall s \tag{26}
$$

$$
\begin{bmatrix} 0 \\ 0 \end{bmatrix} \leq \begin{bmatrix} \xi^{Tot,B,dis}_{t,s} \\ \xi^{Tot,B,ch}_{t,s} \end{bmatrix} \leq \begin{bmatrix} Ca^{B,dis} z^{dis}_t \\ Ca^{B,ch} z^{ch}_t \end{bmatrix} \quad \forall t, \forall s \tag{27}
$$

$$
\begin{bmatrix} 0 \\ 0 \end{bmatrix} \leq \begin{bmatrix} \varpi^D_{t,s} \\ \varpi^{Tot}_{t,s} \end{bmatrix} \leq \lambda \begin{bmatrix} L_{0,t} \\ L_{0,t} \end{bmatrix} \quad \forall t, \forall s \tag{28}
$$

$$0 \leq \xi_{t,s}^{D,W} \leq Ca^{W} \quad \forall t, \forall s \tag{29}$$

$$\xi_{t,s}^{Tot,Sys} = \xi_{t,s}^{Tot,C} + \xi_{t,s}^{Tot,W} + \xi_{t,s}^{Tot,B,dis} + \varpi_{t,s}^{Tot} \quad \forall t, \forall s \tag{30}$$

$$Ca^{A,Sys,se} = \Phi \times (Ca^{C} + Ca^{B,dis} + Ca^{W} + \lambda L_{0,t}) \tag{31}$$

$$Ca^{A,Sys,bu} = \Phi \times (Ca^{B,ch} + Ca^{W}) \tag{32}$$

$$0 \leq \xi_{t,s}^{A,C} + \xi_{t,s}^{A,B,dis} + \xi_{t,s}^{A,W,se} + \varpi_{t,s}^{A} \leq Ca^{A,Sys,se} \quad \forall t, \forall s \tag{33}$$

$$0 \leq \xi_{t,s}^{A,B,ch} + \xi_{t,s}^{A,W,bu} \leq Ca^{A,Sys,bu} \quad \forall t, \forall s \tag{34}$$

$$0 \leq \xi_{t,s}^{Tot,Sys} \leq (Ca^{C}x_{t} + Ca^{B,dis}z_{t}^{dis} + Ca^{W} + \lambda L_{0,t}) \ \forall t, \forall s \tag{35}$$

$$\Lambda_{t,s} = \Lambda_{t,s}^{+} - \Lambda_{t,s}^{-} = P_{t,s}^{W} - \xi_{t,s}^{Tot,W} \quad \forall t, \forall s \tag{36}$$

$$0 \leq \Lambda_{t,s}^{-} \leq (Ca^{C}x_{t} + Ca^{B,dis}z_{t}^{dis} + Ca^{W} + \lambda L_{0,t}) \quad \forall t, \forall s \tag{37}$$

$$0 \leq \Lambda_{t,s}^{+} \leq P_{t,s}^{W} + \xi_{t,s}^{Tot,C} + \xi_{t,s}^{Tot,B,dis} + \varpi_{t,s}^{Tot} \quad \forall t, \forall s \tag{38}$$

(e) Constraints related to constructing offering and bidding curves [34]: The HPGC is obliged to observe the non-decreasing and decreasing conditions for submitting its DA offering and bidding curves. Towards this end, constraints (39) and (40) account for non-decreasing modeling of the DA energy offers; meanwhile, constraint (41) considers the decreasing state of DA energy bids. Lastly, the non-anticipativity provision of the DA and adjustment offering and bidding powers are modeled by (42)-(44).

$$\xi_{t,s}^{D,\theta_1} \leq \xi_{t,\widetilde{s}}^{D,\theta_1}, \quad \forall s, \widetilde{s} : [\varrho_{t,s}^{D} \leq \varrho_{t,\widetilde{s}}^{D}], \quad \forall t \quad \& $$
$$\theta_1 = \left[C, W, (B, dis) \right] \tag{39}$$

14

$$\varpi_{t,s}^D \leq \varpi_{t,\tilde{s}}^D, \quad \forall \omega, \tilde{s} : [\varrho_{t,s}^D \leq \varrho_{t,\tilde{s}}^D], \quad \forall t \tag{40}$$

$$\xi_{t,s}^{D,B,ch} \leq \xi_{t,\tilde{s}}^{D,B,ch}, \quad \forall s, \tilde{s} : [\varrho_{t,s}^D \geq \varrho_{t,\tilde{s}}^D], \quad \forall t \tag{41}$$

$$\xi_{t,s}^{D,\theta_2} = \xi_{t,\tilde{s}}^{D,\theta_2}, \quad \forall s, \tilde{s} : [\varrho_{t,s}^D = \varrho_{t,\tilde{s}}^D], \quad \forall t \quad \&$$
$$\theta_2 = \Big[C, W, (B, dis), (B, ch) \Big] \tag{42}$$

$$\varpi_{t,s}^{\theta_3} = \varpi_{t,\tilde{s}}^{\theta_3}, \quad \forall \omega, \tilde{s} : [\varrho_{t,s}^D = \varrho_{t,\tilde{s}}^D], \quad \forall t \quad \& \quad \theta_3 = [D, A] \tag{43}$$

$$\xi_{t,s}^{A,\theta_2} = \xi_{t,\tilde{s}}^{A,\theta_2}, \quad \forall s, \tilde{s} : [\varrho_{t,s}^D = \varrho_{t,\tilde{s}}^D], \quad \forall t \quad \&$$
$$\theta_2 = \Big[C, (W, se), (W, bu), (B, dis), (B, ch) \Big] \tag{44}$$

3. Reformulate the developed mathematical formulation in the previous step in accordance with the upper boundary of interval numbers ($\overline{EF}_t$ and $\overline{L}_{0,t}$). This reformulation (45a)-(45ar) corresponds to obtaining the upper boundary of the HPGC profit ($\overline{F^{Sys}}$).

$$\overline{F^{Sys}} = \sum_{s=1}^{N_S} \pi_s [\overline{Profit_s^C} + \overline{Profit_s^W} + \overline{Profit_s^B} + \overline{Profit_s^{DR}}] \tag{45a}$$

$$\overline{Profit_s^C} = \sum_{t=1}^{N_T} \varrho_{t,s}^D \overline{\xi_{t,s}^{D,C}} q_t + \varrho_{t,s}^A \overline{\xi_{t,s}^{A,C}} q_t \quad \forall s \tag{45b}$$

$$\overline{Profit_s^W} = \sum_{t=1}^{N_T} \varrho_{t,s}^D \overline{\xi_{t,s}^{D,W}} q_t + \varrho_{t,s}^A \overline{\xi_{t,s}^{A,W,se}} q_t - \varrho_{t,s}^A \overline{\xi_{t,s}^{A,W,bu}} q_t$$
$$+ \left(\varrho_{t,s}^D \iota_{t,s}^+ \overline{\Lambda_{t,s}^+} \right) - \left(\varrho_{t,s}^D \iota_{t,s}^- \overline{\Lambda_{t,s}^-} \right) \quad \forall s \tag{45c}$$

$$\overline{Profit_s^B} = \sum_{t=1}^{N_T} \varrho_{t,s}^D \overline{\xi_{t,s}^{D,B,dis}} q_t - \varrho_{t,s}^D \overline{\xi_{t,s}^{D,B,ch}} q_t + \varrho_{t,s}^A \overline{\xi_{t,s}^{A,B,dis}} q_t - \varrho_{t,s}^A \overline{\xi_{t,s}^{A,B,ch}} q_t \quad \forall s$$
$$\tag{45d}$$

$$\overline{\mathrm{Profit}_s^{\mathrm{DR}}} = \sum_{t=1}^{N_T} \varrho_{t,s}^D \overline{\varpi_{t,s}^D} q_t + \varrho_{t,s}^A \overline{\varpi_{t,s}^A} q_t + \varrho^* \left(\overline{\varpi_{t,s}^D} + \overline{\varpi_{t,s}^A} \right) q_t$$

$$+ \frac{1}{2\varphi \overline{L_{0,t}}} \sum_{b=1}^{N_B} S_b \overline{\varpi_{b,t,s}^{\mathrm{Tot\_b}}} \quad \forall s \qquad (45e)$$

$$\begin{bmatrix} \overline{\xi_{t,s}^{D,C}} \\ \overline{\xi_{t,s}^{A,C}} \end{bmatrix} = \begin{bmatrix} \overline{\xi_{t,s}^{D,SE}} \\ \overline{\xi_{t,s}^{A,SE}} \end{bmatrix} + \begin{bmatrix} \overline{\xi_{t,s}^{D,FE}} \\ \overline{\xi_{t,s}^{A,FE}} \end{bmatrix} \quad \forall t, \forall s \qquad (45f)$$

$$\begin{bmatrix} \overline{\xi_{t,s}^{\mathrm{Tot},C}} \\ \overline{\xi_{t,s}^{\mathrm{Tot},SE}} \\ \overline{\xi_{t,s}^{\mathrm{Tot},FE}} \end{bmatrix} = \begin{bmatrix} \overline{\xi_{t,s}^{D,C}} \\ \overline{\xi_{t,s}^{D,SE}} \\ \overline{\xi_{t,s}^{D,FE}} \end{bmatrix} + \begin{bmatrix} \overline{\xi_{t,s}^{A,C}} \\ \overline{\xi_{t,s}^{A,SE}} \\ \overline{\xi_{t,s}^{A,FE}} \end{bmatrix} \quad \forall t, \forall s \qquad (45g)$$

$$\overline{\xi_{t,s}^{\mathrm{Tot},SE}} = \beta_3 \overline{\varsigma_{t,s}^{SE}} \quad \forall t, \forall s \qquad (45h)$$

$$\overline{\xi_{t,s}^{\mathrm{Tot},FE}} = \beta_1 \overline{\varsigma_{t,s}^{FE}} \quad \forall t, \forall s \qquad (45i)$$

$$\beta_2 \left(\overline{\varsigma_{t+1,s}^{FS}} - \overline{\varsigma_{t,s}^{FS}} \right) \leq \mathrm{RUR}^{\mathrm{ch}} \quad \forall t = 0, \ldots, N_T - 1, \forall s \qquad (45j)$$

$$\overline{\xi_{t,s}^{\mathrm{Tot},SE}} - \overline{\xi_{t+1,s}^{\mathrm{Tot},SE}} \leq \mathrm{RDR}^{\mathrm{dis}} \quad \forall t = 0, \ldots, N_T - 1, \forall s \qquad (45k)$$

$$\overline{\varsigma_{t,s}^{FE}} + \overline{\varsigma_{t,s}^{FS}} \leq \overline{\mathrm{EF}_t} \quad \forall t, \forall s \qquad (45l)$$

$$\varsigma^{E,\mathrm{Min}} x_t \leq \overline{\varsigma_{t,s}^{FE}} + \overline{\varsigma_{t,s}^{SE}} \leq \varsigma^{E,\mathrm{Max}} x_t \quad \forall t, \forall s \qquad (45m)$$

$$\overline{\varsigma_{t,s}^{S}} = \varsigma_0 + \beta_2 \overline{\varsigma_{t,s}^{FS}} - \overline{\varsigma_{t,s}^{SE}} \quad \forall t = 1, \forall s \qquad (45n)$$

$$\overline{\varsigma_{t,s}^{S}} = \overline{\varsigma_{t-1,s}^{S}} + \beta_2 \overline{\varsigma_{t,s}^{FS}} - \overline{\varsigma_{t,s}^{SE}} \quad \forall t \geq 2, \forall s \qquad (45o)$$

$$\varsigma^{S,\mathrm{Min}} \leq \overline{\varsigma_{t,s}^{S}} \leq \varsigma^{S,\mathrm{Max}} \quad \forall t, \forall s \qquad (45p)$$

$$\begin{bmatrix} \overline{\xi_{t,s}^{Tot,B,dis}} \\ \overline{\xi_{t,s}^{Tot,B,ch}} \end{bmatrix} = \begin{bmatrix} \overline{\xi_{t,s}^{D,B,dis}} \\ \overline{\xi_{t,s}^{D,B,ch}} \end{bmatrix} + \begin{bmatrix} \overline{\xi_{t,s}^{A,B,dis}} \\ \overline{\xi_{t,s}^{A,B,ch}} \end{bmatrix} \quad \forall t, \forall s \tag{45q}$$

$$z_t^{dis} + z_t^{ch} \leq 1, \quad \forall t \tag{45r}$$

$$\overline{\varkappa_{t,s}^{B}} = \overline{\varkappa_{t-1,s}^{B}} - \left(\frac{1}{\varepsilon^{B,dis}} \right) \overline{\xi_{t,s}^{Tot,B,dis}} + \varepsilon^{B,ch} \overline{\xi_{t,s}^{Tot,B,ch}} \quad \forall t, \forall s \tag{45s}$$

$$0 \leq \overline{\varkappa_{t,s}^{B}} \leq \varkappa^{B,Max}, \quad \forall t, \forall s \tag{45t}$$

$$\overline{\xi_{t,s}^{Tot,W}} = \overline{\xi_{t,s}^{D,W}} + \overline{\xi_{t,s}^{A,W,se}} - \overline{\xi_{t,s}^{A,W,bu}}, \quad \forall t, \forall s \tag{45u}$$

$$\overline{\varpi_{t,s}^{Tot}} = \overline{\varpi_{t,s}^{D}} + \overline{\varpi_{t,s}^{A}} \quad \forall t, \forall s \tag{45v}$$

$$\overline{\varpi_{t,s}^{Tot}} = \sum_{b=1}^{N_B} \overline{\varpi_{b,t,s}^{Tot\_b}} \quad \forall t, \forall s \tag{45w}$$

$$0 \leq \sum_{t=1}^{N_T} \overline{\varpi_{t,s}^{Tot}} \leq \rho \sum_{t=1}^{N_T} \overline{L_{0,t}} \quad \forall t, \forall s \tag{45x}$$

$$\begin{bmatrix} 0 \\ 0 \end{bmatrix} \leq \begin{bmatrix} \overline{\xi_{t,s}^{D,CS}} \\ \overline{\xi_{t,s}^{Tot,CS}} \end{bmatrix} \leq \begin{bmatrix} Ca^C x_t \\ Ca^C x_t \end{bmatrix} \quad \forall t, \forall s \tag{45y}$$

$$\begin{bmatrix} 0 \\ 0 \end{bmatrix} \leq \begin{bmatrix} \overline{\xi_{t,s}^{D,B,dis}} \\ \overline{\xi_{t,s}^{D,B,ch}} \end{bmatrix} \leq \begin{bmatrix} Ca^{B,dis} z_t^{dis} \\ Ca^{B,ch} z_t^{ch} \end{bmatrix} \quad \forall t, \forall s \tag{45z}$$

$$\begin{bmatrix} 0 \\ 0 \end{bmatrix} \leq \begin{bmatrix} \overline{\xi_{t,s}^{Tot,B,dis}} \\ \overline{\xi_{t,s}^{Tot,B,ch}} \end{bmatrix} \leq \begin{bmatrix} Ca^{B,dis} z_t^{dis} \\ Ca^{B,ch} z_t^{ch} \end{bmatrix} \quad \forall t, \forall s \tag{45aa}$$

$$\begin{bmatrix} 0 \\ 0 \end{bmatrix} \leq \begin{bmatrix} \overline{\varpi_{t,s}^{D}} \\ \overline{\varpi_{t,s}^{Tot}} \end{bmatrix} \leq \lambda \begin{bmatrix} \overline{L_{0,t}} \\ \overline{L_{0,t}} \end{bmatrix} \quad \forall t, \forall s \tag{45ab}$$

$$0 \leq \overline{\xi_{t,s}^{D,W}} \leq Ca^W \quad \forall t, \forall s \tag{45ac}$$

$$\overline{\xi_{t,s}^{Tot,Sys}} = \overline{\xi_{t,s}^{Tot,C}} + \overline{\xi_{t,s}^{Tot,W}} + \overline{\xi_{t,s}^{Tot,B,dis}} + \overline{\varpi_{t,s}^{Tot}} \quad \forall t, \forall s \tag{45ad}$$

$$\overline{Ca^{A,Sys,se}} = \Phi \times (Ca^C + Ca^{B,dis} + Ca^W + \overline{\lambda L_{0,t}}) \tag{45ae}$$

$$Ca^{A,Sys,bu} = \Phi \times (Ca^{B,ch} + Ca^W) \tag{45af}$$

$$0 \leq \overline{\xi_{t,s}^{A,C}} + \overline{\xi_{t,s}^{A,B,dis}} + \overline{\xi_{t,s}^{A,W,se}} + \overline{\varpi_{t,s}^A} \leq \overline{Ca^{A,Sys,se}} \quad \forall t, \forall s \tag{45ag}$$

$$0 \leq \overline{\xi_{t,s}^{A,B,ch}} + \overline{\xi_{t,s}^{A,W,bu}} \leq Ca^{A,Sys,bu} \quad \forall t, \forall s \tag{45ah}$$

$$0 \leq \overline{\xi_{t,s}^{Tot,Sys}} \leq (Ca^C x_t + Ca^{B,dis} z_t^{dis} + Ca^W + \lambda \overline{L_{0,t}}) \ \forall t, \forall s \tag{45ai}$$

$$\overline{\Lambda_{t,s}} = \overline{\Lambda_{t,s}^+} - \overline{\Lambda_{t,s}^-} = P_{t,s}^W - \overline{\xi_{t,s}^{Tot,W}} \quad \forall t, \forall s \tag{45aj}$$

$$0 \leq \overline{\Lambda_{t,s}^-} \leq (Ca^C x_t + Ca^{B,dis} z_t^{dis} + Ca^W + \lambda \overline{L_{0,t}}) \quad \forall t, \forall s \tag{45ak}$$

$$0 \leq \overline{\Lambda_{t,s}^+} \leq P_{t,s}^W + \overline{\xi_{t,s}^{Tot,C}} + \overline{\xi_{t,s}^{Tot,B,dis}} + \overline{\varpi_{t,s}^{Tot}} \quad \forall t, \forall s \tag{45al}$$

$$\overline{\xi_{t,s}^{D,\theta_1}} \leq \overline{\xi_{t,\widetilde{s}}^{D,\theta_1}}, \quad \forall s, \widetilde{s} : [\varrho_{t,s}^D \leq \varrho_{t,\widetilde{s}}^D], \quad \forall t \quad \& $$
$$\theta_1 = \Big[C, W, (B, dis) \Big] \tag{45am}$$

$$\overline{\varpi_{t,s}^D} \leq \overline{\varpi_{t,\widetilde{s}}^D}, \quad \forall \omega, \widetilde{s} : [\varrho_{t,s}^D \leq \varrho_{t,\widetilde{s}}^D], \quad \forall t \tag{45an}$$

$$\overline{\xi_{t,s}^{D,B,ch}} \leq \overline{\xi_{t,\widetilde{s}}^{D,B,ch}}, \quad \forall s, \widetilde{s} : [\varrho_{t,s}^D \geq \varrho_{t,\widetilde{s}}^D], \quad \forall t \tag{45ao}$$

$$\overline{\xi_{t,s}^{D,\theta_2}} = \overline{\xi_{t,\widetilde{s}}^{D,\theta_2}}, \quad \forall s, \widetilde{s} : [\varrho_{t,s}^D = \varrho_{t,\widetilde{s}}^D], \quad \forall t \quad \& $$
$$\theta_2 = \Big[C, W, (B, dis), (B, ch) \Big] \tag{45ap}$$

$$\overline{\varpi_{t,s}^{\theta_3}} = \overline{\varpi_{t,\tilde{s}}^{\theta_3}}, \quad \forall \omega, \tilde{s} : [\varrho_{t,s}^{D} = \varrho_{t,\tilde{s}}^{D}], \quad \forall t \ \& \ \theta_3 = [D, A] \tag{45aq}$$

$$\overline{\xi_{t,s}^{A,\theta_2}} = \overline{\xi_{t,\tilde{s}}^{A,\theta_2}}, \quad \forall s, \tilde{s} : [\varrho_{t,s}^{D} = \varrho_{t,\tilde{s}}^{D}], \quad \forall t \ \&$$
$$\theta_2 = \Big[C, (W, se), (W, bu), (B, dis), (B, ch) \Big] \tag{45ar}$$

In order to obtain the mathematical formulation (45a)-(45ar), we need to apply the following changes to the formulas given in (45a)-(45ar):

(a) All interval parameters must be replaced with their upper boundaries, i.e., $\overline{EF}_t$ and $\overline{L}_{0,t}$. Given the theorem proposed in [38] and its implementation in our study, the upper boundary of the objective function is related to a state in which both interval parameters are at their upper boundaries, i.e., $\overline{EF}_t$ and $\overline{L}_{0,t}$

(b) No changes must be applied to binary variables.

(c) All nonbinary variables must be replaced with new variables denoting their upper boundaries, namely, $\overline{(.)}$.

Note that the explanations of formulas (45a)-(45ar) are similar to those of (1)-(44).

4. Reformulate the developed mathematical formulation in step 2 in accordance with the lower boundary of interval numbers ($\underline{EF}_t$ and $\underline{L}_{0,t}$). This reformulation (46a)-(46ar) corresponds to obtaining the lower boundary of the HPGC profit ($\underline{F^{Sys}}$).

$$\underline{F^{Sys}} = \sum_{s=1}^{N_S} \pi_s [\underline{Profit_s^{C}} + \underline{Profit_s^{W}} + \underline{Profit_s^{B}} + \underline{Profit_s^{DR}}] \tag{46a}$$

$$\underline{Profit_s^{C}} = \sum_{t=1}^{N_T} \varrho_{t,s}^{D} \underline{\xi_{t,s}^{D,C}} q_t + \varrho_{t,s}^{A} \underline{\xi_{t,s}^{A,C}} q_t \quad \forall s \tag{46b}$$

$$\underline{Profit_s^{W}} = \sum_{t=1}^{N_T} \varrho_{t,s}^{D} \underline{\xi_{t,s}^{D,W}} q_t + \varrho_{t,s}^{A} \underline{\xi_{t,s}^{A,W,se}} q_t - \varrho_{t,s}^{A} \underline{\xi_{t,s}^{A,W,bu}} q_t$$
$$+ \left(\varrho_{t,s}^{D} \iota_{t,s}^{+} \underline{\Lambda_{t,s}^{+}} \right) - \left(\varrho_{t,s}^{D} \iota_{t,s}^{-} \underline{\Lambda_{t,s}^{-}} \right) \quad \forall s \tag{46c}$$

19

$$\underline{\text{Profit}_s^B} = \sum_{t=1}^{N_T} \varrho_{t,s}^D \underline{\xi_{t,s}^{D,B,\text{dis}}} q_t - \varrho_{t,s}^D \underline{\xi_{t,s}^{D,B,\text{ch}}} q_t + \varrho_{t,s}^A \underline{\xi_{t,s}^{A,B,\text{dis}}} q_t - \varrho_{t,s}^A \underline{\xi_{t,s}^{A,B,\text{ch}}} q_t \quad \forall s$$

(46d)

$$\underline{\text{Profit}_s^{DR}} = \sum_{t=1}^{N_T} \varrho_{t,s}^D \underline{\varpi_{t,s}^D} q_t + \varrho_{t,s}^A \underline{\varpi_{t,s}^A} q_t + \varrho^* \left(\underline{\varpi_{t,s}^D} + \underline{\varpi_{t,s}^A} \right) q_t$$
$$+ \frac{1}{2\varphi \underline{L_{0,t}}} \sum_{b=1}^{N_B} S_b \underline{\varpi_{b,t,s}^{\text{Tot\_b}}} \quad \forall s$$

(46e)

$$\begin{bmatrix} \underline{\xi_{t,s}^{D,C}} \\ \underline{\xi_{t,s}^{A,C}} \end{bmatrix} = \begin{bmatrix} \underline{\xi_{t,s}^{D,SE}} \\ \underline{\xi_{t,s}^{A,SE}} \end{bmatrix} + \begin{bmatrix} \underline{\xi_{t,s}^{D,FE}} \\ \underline{\xi_{t,s}^{A,FE}} \end{bmatrix} \quad \forall t, \forall s$$

(46f)

$$\begin{bmatrix} \underline{\xi_{t,s}^{\text{Tot},C}} \\ \underline{\xi_{t,s}^{\text{Tot},SE}} \\ \underline{\xi_{t,s}^{\text{Tot},FE}} \end{bmatrix} = \begin{bmatrix} \underline{\xi_{t,s}^{D,C}} \\ \underline{\xi_{t,s}^{D,SE}} \\ \underline{\xi_{t,s}^{D,FE}} \end{bmatrix} + \begin{bmatrix} \underline{\xi_{t,s}^{A,C}} \\ \underline{\xi_{t,s}^{A,SE}} \\ \underline{\xi_{t,s}^{A,FE}} \end{bmatrix} \quad \forall t, \forall s$$

(46g)

$$\underline{\xi_{t,s}^{\text{Tot},SE}} = \beta_3 \underline{\varsigma_{t,s}^{SE}} \quad \forall t, \forall s$$

(46h)

$$\underline{\xi_{t,s}^{\text{Tot},FE}} = \beta_1 \underline{\varsigma_{t,s}^{FE}} \quad \forall t, \forall s$$

(46i)

$$\beta_2 \left(\underline{\varsigma_{t+1,s}^{FS}} - \underline{\varsigma_{t,s}^{FS}} \right) \leq \text{RUR}^{\text{ch}} \quad \forall t = 0, \dots, N_T - 1, \forall s$$

(46j)

$$\underline{\xi_{t,s}^{\text{Tot},SE}} - \underline{\xi_{t+1,s}^{\text{Tot},SE}} \leq \text{RDR}^{\text{dis}} \quad \forall t = 0, \dots, N_T - 1, \forall s$$

(46k)

$$\underline{\varsigma_{t,s}^{FE}} + \underline{\varsigma_{t,s}^{FS}} \leq \underline{\text{EF}_t} \quad \forall t, \forall s$$

(46l)

$$\varsigma^{E,\text{Min}} x_t \leq \underline{\varsigma_{t,s}^{FE}} + \underline{\varsigma_{t,s}^{SE}} \leq \varsigma^{E,\text{Max}} x_t \quad \forall t, \forall s$$

(46m)

$$\underline{\varsigma_{t,s}^{S}} = \varsigma_0 + \beta_2 \underline{\varsigma_{t,s}^{FS}} - \underline{\varsigma_{t,s}^{SE}} \quad \forall t = 1, \forall s$$

(46n)

20

$$\underline{\varsigma_{t,s}^{S}} = \underline{\varsigma_{t-1,s}^{S}} + \beta_2 \underline{\varsigma_{t,s}^{FS}} - \underline{\varsigma_{t,s}^{SE}} \quad \forall t \geq 2, \forall s \tag{46o}$$

$$\varsigma^{S,Min} \leq \underline{\varsigma_{t,s}^{S}} \leq \varsigma^{S,Max} \quad \forall t, \forall s \tag{46p}$$

$$\begin{bmatrix} \underline{\xi_{t,s}^{Tot,B,dis}} \\ \underline{\xi_{t,s}^{Tot,B,ch}} \end{bmatrix} = \begin{bmatrix} \underline{\xi_{t,s}^{D,B,dis}} \\ \underline{\xi_{t,s}^{D,B,ch}} \end{bmatrix} + \begin{bmatrix} \underline{\xi_{t,s}^{A,B,dis}} \\ \underline{\xi_{t,s}^{A,B,ch}} \end{bmatrix} \quad \forall t, \forall s \tag{46q}$$

$$z_t^{dis} + z_t^{ch} \leq 1, \quad \forall t \tag{46r}$$

$$\underline{\varkappa_{t,s}^{B}} = \underline{\varkappa_{t-1,s}^{B}} - \left(\frac{1}{\varepsilon^{B,dis}} \right) \underline{\xi_{t,s}^{Tot,B,dis}} + \varepsilon^{B,ch} \underline{\xi_{t,s}^{Tot,B,ch}} \quad \forall t, \forall s \tag{46s}$$

$$0 \leq \underline{\varkappa_{t,s}^{B}} \leq \varkappa^{B,Max}, \quad \forall t, \forall s \tag{46t}$$

$$\underline{\xi_{t,s}^{Tot,W}} = \underline{\xi_{t,s}^{D,W}} + \underline{\xi_{t,s}^{A,W,se}} - \underline{\xi_{t,s}^{A,W,bu}}, \quad \forall t, \forall s \tag{46u}$$

$$\underline{\varpi_{t,s}^{Tot}} = \underline{\varpi_{t,s}^{D}} + \underline{\varpi_{t,s}^{A}} \quad \forall t, \forall s \tag{46v}$$

$$\underline{\varpi_{t,s}^{Tot}} = \sum_{b=1}^{N_B} \underline{\varpi_{b,t,s}^{Tot\_b}} \quad \forall t, \forall s \tag{46w}$$

$$0 \leq \sum_{t=1}^{N_T} \underline{\varpi_{t,s}^{Tot}} \leq \rho \sum_{t=1}^{N_T} \underline{L_{0,t}} \quad \forall t, \forall s \tag{46x}$$

$$\begin{bmatrix} 0 \\ 0 \end{bmatrix} \leq \begin{bmatrix} \underline{\xi_{t,s}^{D,CS}} \\ \underline{\xi_{t,s}^{Tot,CS}} \end{bmatrix} \leq \begin{bmatrix} Ca^C x_t \\ Ca^C x_t \end{bmatrix} \quad \forall t, \forall s \tag{46y}$$

$$\begin{bmatrix} 0 \\ 0 \end{bmatrix} \leq \begin{bmatrix} \underline{\xi_{t,s}^{D,B,dis}} \\ \underline{\xi_{t,s}^{D,B,ch}} \end{bmatrix} \leq \begin{bmatrix} Ca^{B,dis} z_t^{dis} \\ Ca^{B,ch} z_t^{ch} \end{bmatrix} \quad \forall t, \forall s \tag{46z}$$

$$
\begin{bmatrix} 0 \\ 0 \end{bmatrix} \leq \begin{bmatrix} \underline{\xi_{t,s}^{Tot,B,dis}} \\ \underline{\xi_{t,s}^{Tot,B,ch}} \end{bmatrix} \leq \begin{bmatrix} Ca^{B,dis}z_t^{dis} \\ Ca^{B,ch}z_t^{ch} \end{bmatrix} \quad \forall t, \forall s \tag{46aa}
$$

$$
\begin{bmatrix} 0 \\ 0 \end{bmatrix} \leq \begin{bmatrix} \underline{\varpi_{t,s}^{D}} \\ \underline{\varpi_{t,s}^{Tot}} \end{bmatrix} \leq \lambda \begin{bmatrix} \underline{L_{0,t}} \\ \underline{L_{0,t}} \end{bmatrix} \quad \forall t, \forall s \tag{46ab}
$$

$$
0 \leq \underline{\xi_{t,s}^{D,W}} \leq Ca^{W} \quad \forall t, \forall s \tag{46ac}
$$

$$
\underline{\xi_{t,s}^{Tot,Sys}} = \underline{\xi_{t,s}^{Tot,C}} + \underline{\xi_{t,s}^{Tot,W}} + \underline{\xi_{t,s}^{Tot,B,dis}} + \underline{\varpi_{t,s}^{Tot}} \quad \forall t, \forall s \tag{46ad}
$$

$$
\underline{Ca^{A,Sys,se}} = \Phi \times (Ca^{C} + Ca^{B,dis} + Ca^{W} + \underline{\lambda L_{0,t}}) \tag{46ae}
$$

$$
Ca^{A,Sys,bu} = \Phi \times (Ca^{B,ch} + Ca^{W}) \tag{46af}
$$

$$
0 \leq \underline{\xi_{t,s}^{A,C}} + \underline{\xi_{t,s}^{A,B,dis}} + \underline{\xi_{t,s}^{A,W,se}} + \underline{\varpi_{t,s}^{A}} \leq \underline{Ca^{A,Sys,se}} \quad \forall t, \forall s \tag{46ag}
$$

$$
0 \leq \underline{\xi_{t,s}^{A,B,ch}} + \underline{\xi_{t,s}^{A,W,bu}} \leq Ca^{A,Sys,bu} \quad \forall t, \forall s \tag{46ah}
$$

$$
0 \leq \underline{\xi_{t,s}^{Tot,Sys}} \leq (Ca^{C}x_t + Ca^{B,dis}z_t^{dis} + Ca^{W} + \lambda\underline{L_{0,t}}) \ \forall t, \forall s \tag{46ai}
$$

$$
\underline{\Lambda_{t,s}} = \underline{\Lambda_{t,s}^{+}} - \underline{\Lambda_{t,s}^{-}} = P_{t,s}^{W} - \underline{\xi_{t,s}^{Tot,W}} \quad \forall t, \forall s \tag{46aj}
$$

$$
0 \leq \underline{\Lambda_{t,s}^{-}} \leq (Ca^{C}x_t + Ca^{B,dis}z_t^{dis} + Ca^{W} + \lambda\underline{L_{0,t}}) \quad \forall t, \forall s \tag{46ak}
$$

$$
0 \leq \underline{\Lambda_{t,s}^{+}} \leq P_{t,s}^{W} + \underline{\xi_{t,s}^{Tot,C}} + \underline{\xi_{t,s}^{Tot,B,dis}} + \underline{\varpi_{t,s}^{Tot}} \quad \forall t, \forall s \tag{46al}
$$

$$
\underline{\xi_{t,s}^{D,\theta_1}} \leq \underline{\xi_{t,\widetilde{s}}^{D,\theta_1}}, \quad \forall s, \widetilde{s} : [\varrho_{t,s}^{D} \leq \varrho_{t,\widetilde{s}}^{D}], \quad \forall t \quad \&
$$
$$
\theta_1 = \left[C, W, (B, dis) \right] \tag{46am}
$$

$$\underline{\varpi^{\mathrm{D}}_{t,s}} \leq \underline{\varpi^{\mathrm{D}}_{t,\widetilde{s}}}, \quad \forall \omega, \widetilde{s} : [\varrho^{\mathrm{D}}_{t,s} \leq \varrho^{\mathrm{D}}_{t,\widetilde{s}}], \quad \forall t \tag{46an}$$

$$\underline{\xi^{\mathrm{D,B,ch}}_{t,s}} \leq \underline{\xi^{\mathrm{D,B,ch}}_{t,\widetilde{s}}}, \quad \forall s, \widetilde{s} : [\varrho^{\mathrm{D}}_{t,s} \geq \varrho^{\mathrm{D}}_{t,\widetilde{s}}], \quad \forall t \tag{46ao}$$

$$\underline{\xi^{\mathrm{D},\theta_2}_{t,s}} = \underline{\xi^{\mathrm{D},\theta_2}_{t,\widetilde{s}}}, \quad \forall s, \widetilde{s} : [\varrho^{\mathrm{D}}_{t,s} = \varrho^{\mathrm{D}}_{t,\widetilde{s}}], \quad \forall t \quad \&$$
$$\theta_2 = \Big[\mathrm{C}, \mathrm{W}, (\mathrm{B, dis}), (\mathrm{B, ch}) \Big] \tag{46ap}$$

$$\underline{\varpi^{\theta_3}_{t,s}} = \underline{\varpi^{\theta_3}_{t,\widetilde{s}}}, \quad \forall \omega, \widetilde{s} : [\varrho^{\mathrm{D}}_{t,s} = \varrho^{\mathrm{D}}_{t,\widetilde{s}}], \quad \forall t \quad \& \quad \theta_3 = [\mathrm{D, A}] \tag{46aq}$$

$$\underline{\xi^{\mathrm{A},\theta_2}_{t,s}} = \underline{\xi^{\mathrm{A},\theta_2}_{t,\widetilde{s}}}, \quad \forall s, \widetilde{s} : [\varrho^{\mathrm{D}}_{t,s} = \varrho^{\mathrm{D}}_{t,\widetilde{s}}], \quad \forall t \quad \&$$
$$\theta_2 = \Big[\mathrm{C}, (\mathrm{W, se}), (\mathrm{W, bu}), (\mathrm{B, dis}), (\mathrm{B, ch}) \Big] \tag{46ar}$$

The following modifications have to be made to the formulas in (1)-(44) in order to obtain the mathematical formulation (46a)-(46ar).

(a) All interval parameters must be replaced with their lower boundaries, i.e., $\underline{\mathrm{EF}}_t$ and $\underline{\mathrm{L}}_{0,t}$. Given the theorem proposed in [38] and its implementation in our study, the lower boundary of the objective function is related to a state in which both interval parameters are at their lower boundaries, i.e., $\underline{\mathrm{EF}}_t$ and $\underline{\mathrm{L}}_{0,t}$

(b) No changes must be applied to binary variables.

(c) All nonbinary variables must be replaced with new variables denoting their lower boundaries, namely, $\underline{(.)}$.

Note that the formulas (46a)-(46ar) describe the same property as the formulas (1)-(44).

5. Develop the expected radius and midpoint of the objective function, i.e., $\mathrm{F}^{\mathrm{Sys,r}}$ and $\mathrm{F}^{\mathrm{Sys,m}}$, respectively, based on the following formulas.

$$\mathrm{F}^{\mathrm{Sys,r}} = \frac{\overline{\mathrm{F}^{\mathrm{Sys}}} - \underline{\mathrm{F}^{\mathrm{Sys}}}}{2} \tag{47}$$

$$\mathrm{F}^{\mathrm{Sys,m}} = \frac{\overline{\mathrm{F}^{\mathrm{Sys}}} + \underline{\mathrm{F}^{\mathrm{Sys}}}}{2} \tag{48}$$

where $\mathrm{F}^{\mathrm{Sys,r}}$ shows the expected risk faced by the HPGC due to the interval numbers and $\mathrm{F}^{\mathrm{Sys,m}}$ expresses its expected average profit.

23

6. Incorporate the risk caused by the stochastic scenarios by means of the CVaR criterion into the proposed methodology. To do so, the CVaR objective function (49) and its relevant constraints (50)-(51) are included in the foregoing model.

$$\text{CVaR} = \sigma - \frac{1}{1-\alpha} \sum_{s=1}^{N_S} \pi_s \epsilon_s \tag{49}$$

$$-\text{Profit}_s^{C,m} - \text{Profit}_s^{W,m} - \text{Profit}_s^{B,m} - \text{Profit}_s^{DR,m} + \sigma - \epsilon_s \leq 0 \quad \forall s \tag{50}$$

$$\epsilon_s \geq 0, \quad \forall s \tag{51}$$

where σ and ϵ_s are supplementary variables employed for CVaR computation and α stands for the confidence level.

7. The final risk-based MSI architecture is a mathematical programming problem with three objective functions as follows:

$$\begin{aligned} &\text{Maximize } F^{Sys,m} \\ &\text{Minimize } F^{Sys,r} \\ &\text{Maximize } \text{CVaR} \end{aligned} \tag{52}$$

The set of constraints for these objective functions include:

$$\text{Constraints } (45a) - (45ar), \ (46a) - (46ar), \ (47) - (51) \tag{53}$$

$$\begin{aligned} \beta_2 \left(\underline{\varsigma_{t+1,s}^{FS}} - \overline{\varsigma_{t,s}^{FS}} \right) &\leq \text{RUR}^{ch} \quad \forall t = 0, \ldots, N_T - 1, \forall s \\ \beta_2 \left(\overline{\varsigma_{t+1,s}^{FS}} - \underline{\varsigma_{t,s}^{FS}} \right) &\leq \text{RUR}^{ch} \quad \forall t = 0, \ldots, N_T - 1, \forall s \\ \underline{\xi_{t,s}^{Tot,SE}} - \overline{\xi_{t+1,s}^{Tot,SE}} &\leq \text{RDR}^{dis} \quad \forall t = 0, \ldots, N_T - 1, \forall s \\ \overline{\xi_{t,s}^{Tot,SE}} - \underline{\xi_{t+1,s}^{Tot,SE}} &\leq \text{RDR}^{dis} \quad \forall t = 0, \ldots, N_T - 1, \forall s \end{aligned} \tag{54}$$

Note that the set of constraints (54) are added to the previously developed constraints to avoid impractical CSP's ramping materializations. To obtain the Pareto frontier of the developed mathematical programming problem (52)-(54), both NBI technique and lexicographic optimization are adopted [39].
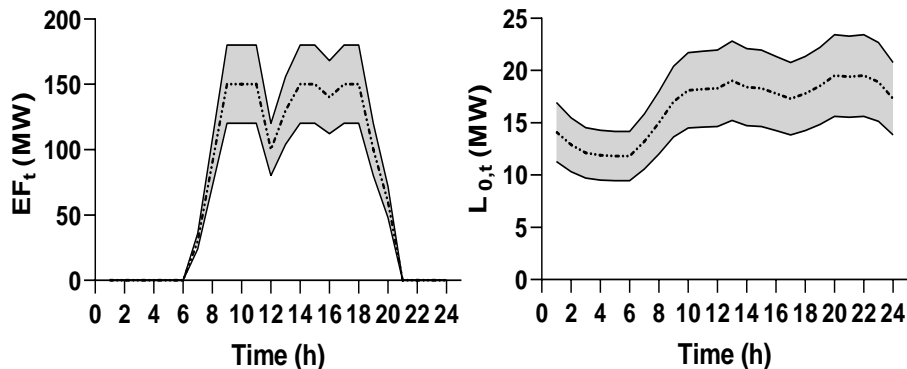
Figure 2: Daily forecast of interval parameters with ±20% uncertainty interval.

3. Case Study

3.1. Data

The test system is an HPGC with a 50 MW CSP system, a 50 MW wind power plant, a battery system with 50 MW power and 250 MWh storage, and lastly, a DRP. It is noteworthy to say that the examined CSP system in this work is quite similar to that tested in [9]. Both interval parameters, namely, DRP's load before load shedding and thermal power of the CSP's solar field, are shown in Fig. 2. Parameters $\varepsilon^{\mathrm{B,dis}}$, $\varepsilon^{\mathrm{B,ch}}$, ϱ^*, α [40], ρ, λ, φ, and Φ are set to 0.95, 0.8, 0.3, 0.95, 0.04, 0.2, -0.3, and 0.3, respectively.

Towards the intended three-stage decision-making model, we need to extract the stochastic scenarios of the wind speed and market parameters. Following this, the hourly data of the aforementioned parameters for a specific period (e.g., in this paper, the first six months of 2018) are collected [41]-[42]. Subsequently, similar to [32], plenty of scenarios are made and then reduced to finally attain a scenario tree with 625 scenarios, meaning that each stochastic parameter has five scenarios. The elaborated mixed-integer programming model is coded in GAMS and solved via CPLEX with a relative gap equal to zero.
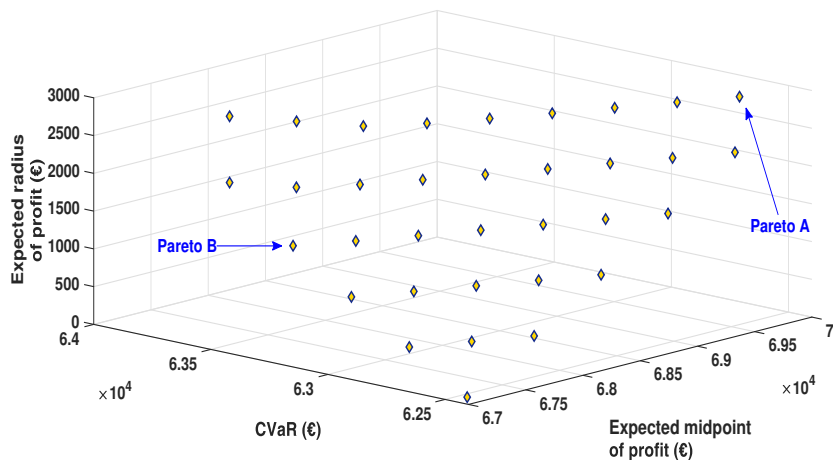
Figure 3: The set of Pareto solutions of the proposed hybrid stochastic-interval architecture for $\pm 10\%$ uncertainty interval.

3.2. Results

The suggested risk-based hybrid stochastic-interval architecture by adopting lexicographic optimization and NBI-technique is executed. As stated in Section 2, the proposed methodology embraces three objective functions, whereby $\mathrm{F^{Sys,m}}(q,i)$ tackles the profit maximization and $\mathrm{F^{Sys,r}}(q,i)$ and CVaR serve as risk management tools. The Pareto sets obtained for the considered methodology for $\pm 10\%$ and $\pm 20\%$ uncertainty intervals are depicted in Fig. 3 and Fig. 4, while any of the axes represents the aforesaid objective functions' values. We observe that for the higher uncertainty intervals, the risk associated with interval numbers, i.e., expected radius of profit, covers a broader range. Simply put, greater uncertainty intervals increase the risk of decision-making, as expected.

According to Fig. 3 and Fig. 4, a set of different solutions, representing various levels of risk and financial profit, is obtained through the proposed MSI model. Accordingly, any specific solution with the desired level of risk and profit can be chosen by the decision-maker as its final operating strategy. To investigate the characteristics of different solutions obtained by the proposed MSI methodology, two distinct operating strategies, i.e., Pareto A and Pareto
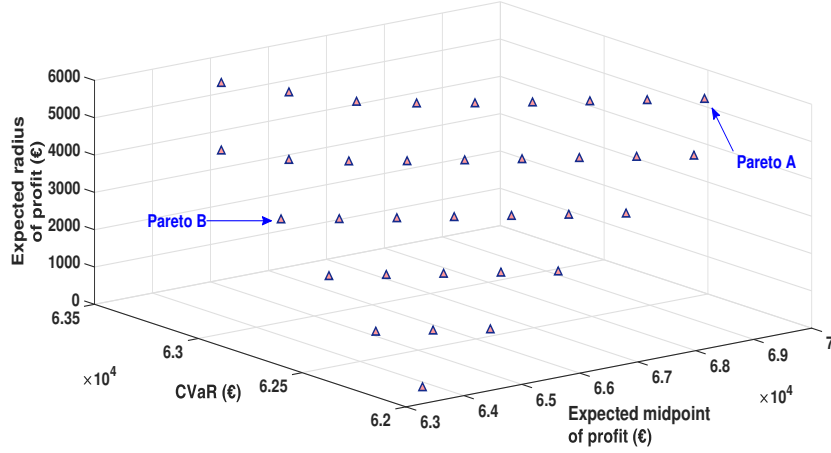
26

Figure 4: The set of Pareto solutions of the proposed hybrid stochastic-interval architecture for $\pm 20\%$ uncertainty interval.

Table 1: Profit intervals of the HPGC for two operating strategies.

Strategy	Lower bound ($\mathcal{E}$)	Upper bound ($\mathcal{E}$)	Midpoint ($\mathcal{E}$)
Pareto A ($\pm 10\%$)	67,130.440	72,686.903	69,908.671
Pareto B ($\pm 10\%$)	67,040.826	68,885.112	67,962.969
Pareto A ($\pm 20\%$)	63,801.010	75,071.993	69,436.502
Pareto B ($\pm 20\%$)	63,579.305	67,364.783	65,472.044

B, have been selected, as shown in Fig. 3 and Fig. 4. A comparison between the characteristics of these two operating strategies can be summarized as:

$$\mathrm{F}^{\mathrm{Sys,m}}(A) \geq \mathrm{F}^{\mathrm{Sys,m}}(B), \quad \mathrm{F}^{\mathrm{Sys,r}}(A) \geq \mathrm{F}^{\mathrm{Sys,r}}(B),$$

$$\mathrm{CVaR}(A) \leq \mathrm{CVaR}(B)$$

From the above, it can be interpreted that higher $\mathrm{F}^{\mathrm{Sys,m}}$ and $\mathrm{F}^{\mathrm{Sys,r}}$ and lower CVaR of Pareto A denotes it as an optimistic operating model, whereas Pareto B symbolizes a pessimistic one. It is not pointless to state that the higher the CVaR, the lower the risk. Correspondingly, the lower the expected radius of

27

Table 2: Model's performance and statistics

Laptop computer [RAM= 8 GB, Processor=Core i5 @ 2.30 GHz]	
# of continuous variables	13,725
# of binary variables	120
# of equations variables	19,006
Computation time [Pareto A ($\pm 10\%$)]	20.8 Sec
Computation time [Pareto B ($\pm 10\%$)]	33.2 Sec
Computation time [Pareto A ($\pm 20\%$)]	75.4 Sec
Computation time [Pareto B ($\pm 20\%$)]	99.8 Sec

profit, the more conservative the HPGC. From now on, Pareto A and B refer to optimistic and pessimistic operating strategies, respectively. Table 1 reports the comparison results of the optimistic and pessimistic operating strategies in terms of the profit intervals. As shown in Table 1, the maximum quantities of the upper and lower boundaries are obtained for greater and smaller prediction intervals of the interval numbers, respectively. In contrast, the minimum values of the upper and lower boundaries are achieved for smaller and greater prediction intervals, respectively. Furthermore, to realize pessimistic operating states, the proposed methodology lessens the profit intervals, and as a result, the radius of the profit decreases. The model's performance and statistics are reported in Table 2.

The optimistic and pessimistic bidding curves of the battery in the DA market for two sample hours have been compared in Fig. 5a, while Fig. 5b provides its offering curves. In addition, Fig. 6a and Fig. 6b display the offering behavior of the CSP system and wind turbines in the DA market from the optimistic and pessimistic perspectives. It is necessary to mention that, in these figures, the midpoint values of output variables are exploited to compare optimistic and
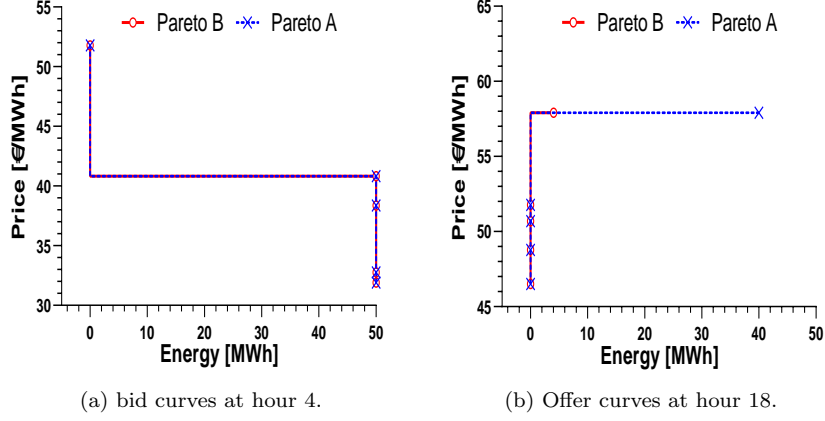
(a) bid curves at hour 4.

(b) Offer curves at hour 18.

Figure 5: Effects of optimistic and pessimistic strategies on submitting curves of the battery in the DA market.

(a) CSP system at hour 18.

(b) Wind turbines at hour 18.
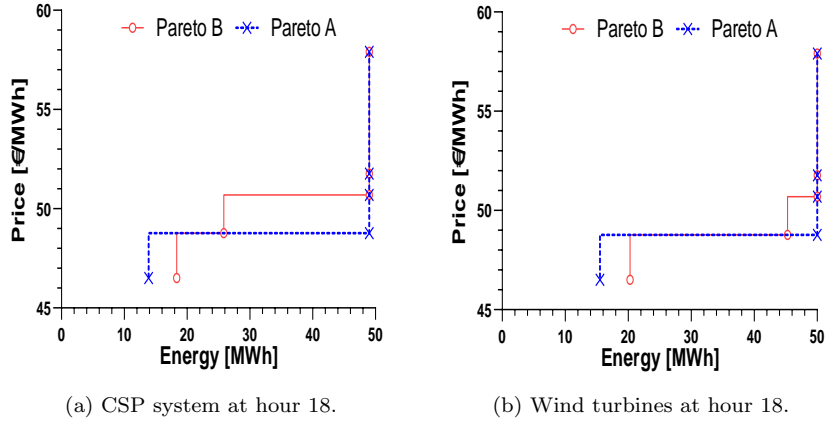
Figure 6: Effects of optimistic and pessimistic strategies on submitting offering curves of the CSP system and wind turbines in the DA market.

pessimistic actions. These midpoint values are obtained similar to what was introduced for the midpoint of the objective function in Eq. (48). According to Fig. 5a, we perceive that the bidding strategy of the battery at hour 4 is not affected by optimistic or pessimistic actions. Conversely, in the optimistic strategy, a significant increment in the offering value of the battery for the highest

29

Table 3: Commitment status of the battery system and the CSP unit.

Unit	Strategy	Hours (1-24)
Battery	Pareto A (±20%)	222222211111210021111100
	Pareto B (±20%)	2222222111112**2**0**1**1111**11**
CSP	Pareto A (±20%)	000000111111111111111111
	Pareto B (±20%)	000000111111111111111111

Note ⇒ For Battery: 1, 2, and 0 stand for discharging, charging, and offline statuses, respectively; For CSPP: 1 and 0 indicate online and offline statuses, respectively.

DA price materialization at hour 18 is seen compared to the pessimistic one. From figure 5, the effect of optimistic and pessimistic operating strategies can only be discerned at the lowest DA price realizations, namely, 48.77 and 46.51 €/MWh.

The influence of different operating strategies on the commitment status of the battery and the CSP unit has been illustrated in Table 3. As the operating strategy changes, the commitment states of the battery alters at hours 14, 15, 17, 23, and 24. By contrast, no alteration in the commitment status of the CSP unit occurs by changing the HPGC approach. The CSP unit is offline during the first six hours owing to zero solar irradiation, while it starts running at hour 7 and remains online for the rest of the day on account of the available solar energy and embedded thermal energy storage. To sum up, the flexibility of a unit has a direct impact on its commitment status under various operating strategies.

The hourly transacted DA and adjustment energy, as well as the overall real-time deviation of the HPGC for both designated optimistic and pessimistic operating strategies, have been depicted in Fig. 7, Fig. 8, and Fig. 9, respectively. It can be seen from Fig. 7 that, for the peak periods, the HPGC possesses greater hourly intervals of the transacted DA energy in the optimistic strategy, whereas wider intervals during the off-peak periods are experienced in
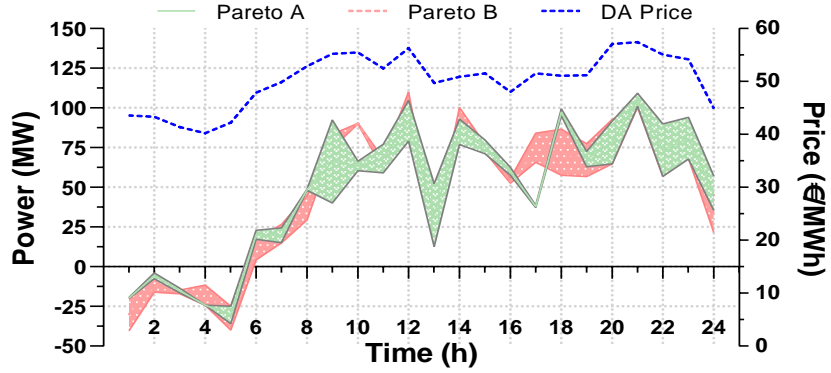
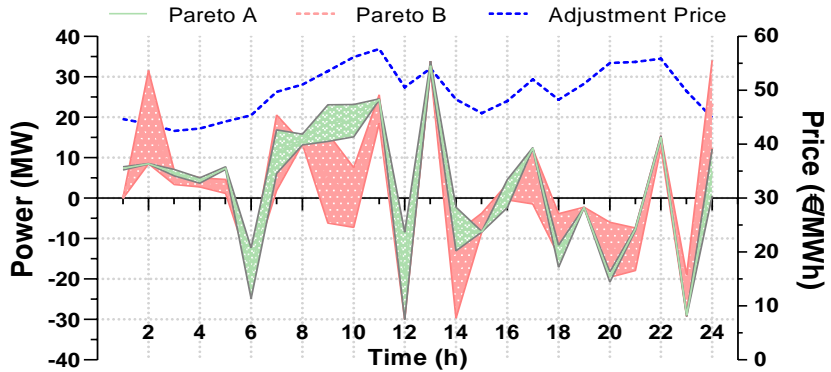Figure 7: The hourly intervals of the transacted DA energy of the entire system under ±20% uncertainty interval.

Figure 8: The hourly intervals of the transacted adjustment energy of the entire system under ±20% uncertainty interval.

the pessimistic one. On the other hand, as can be observed from the overall trend in Fig. 8, wider intervals of the hourly transacted adjustment energy are observed for the risk-mitigating strategy. The reason lies in dropping the overall deviation of the HPGC in the real-time market by further exploiting the adjustment market. This issue is shown in Fig. 9. As the HPGC goes toward the pessimistic strategy, the hourly intervals of the overall deviation in the real-time market grow narrower. Following the above, the total daily intervals of the aforementioned variables are exhibited in Fig. 10. The midpoint of the daily transacted energy in the DA market for both risk-involved strategies
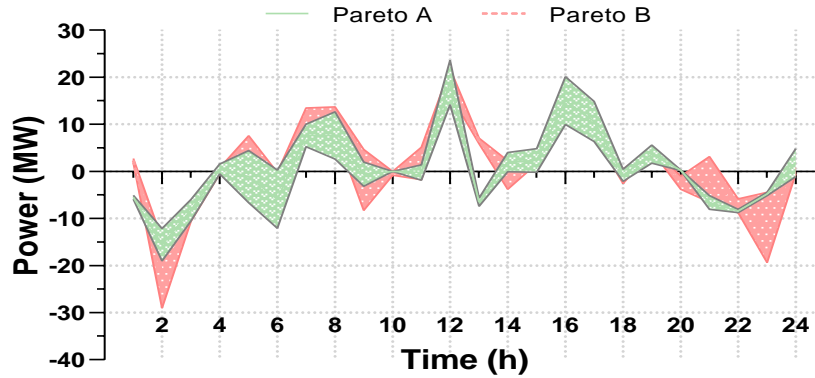
Figure 9: The hourly intervals of the overall real-time deviation under $\pm20\%$ uncertainty interval.

is approximately equal, while the optimistic action possesses wider intervals. Moreover, the midpoint of the daily transacted energy in the adjustment market in the optimistic strategy is greater than the pessimistic one, meaning that the system's attention in the pessimistic behavior is further on buying energy rather than selling it. Eventually, the larger midpoint of the overall real-time deviation in the pessimistic operating strategy reveals that the system's trend in the risk-mitigating strategy is to increase its total positive deviation, hoping to lower its risk at this market.

4. Conclusions

In this work, an MSI methodology was proposed to efficaciously tackle the operating strategy problem of a CSP unit, a battery system, wind turbines, and a DRP, focusing on the DA and adjustment markets, while the owner of the aforementioned resources was the HPGC. The elaborated MSI methodology aimed at covering drastic uncertainty origins, including market parameters, wind generation, DRP's load, and the thermal power of the CSP's solar field. The proposed innovative MSI framework was run under a multi-objective programming structure. By testing the proposed setup using two case studies, it was found that: 1) The risk preference of the decision-maker concerning inter-
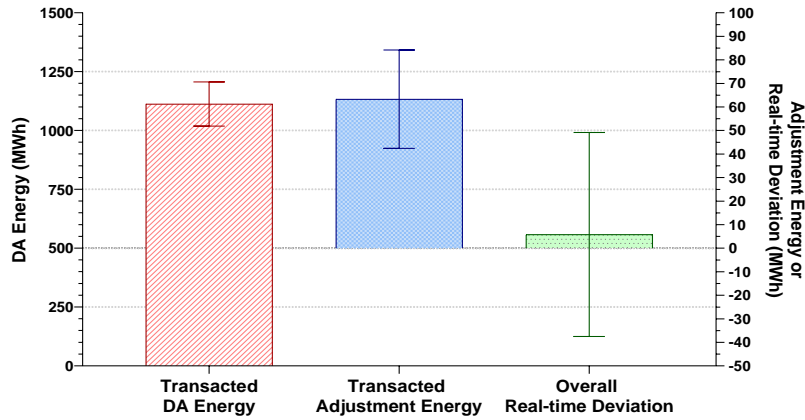
(a) Pareto A (Optimistic)
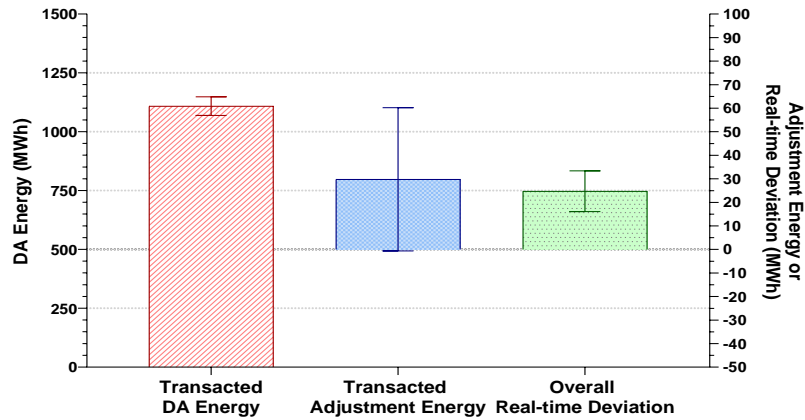
(b) Pareto B (Pessimistic)

Figure 10: The intervals of the daily transacted DA and adjustment energy as well as daily overall real-time deviation under $\pm 20\%$ forecasting error.

val and stochastic parameters can be efficiently handled using the suggested methodology, 2) As the forecasting error of interval parameters increases, the risk criterion associated with these parameters covers a broader scope, 3) The risk related to interval numbers is lessened by means of lowering the interval of the objective function, 4) The commitment status of the battery is further subordinate to the risk preference of the HPGC compared to the CSP unit ow-

ing to less technical operating constraints, 5) As the conservatism of the HPGC increases, the interval of the total transacted DA energy decreases. At the same time, further participation in the adjustment market is exploited to lessen the interval of overall real-time deviations. Future work will address the following aspects: 1) Presenting a comprehensive risk assessment study on the existing risk-controlling models, 2) Investigating the role of ancillary service markets on the profitability of the considered HPGC, and 3) Examining the impact of strategic reserve purchasing to cope with imbalances caused by wind generation in the developed framework.

Nomenclature

Indices

b	Blocks' slope index, 1 to N_B.
s	Scenarios index, 1 to N_S.
t	Periods index, 1 to N_T.

Superscripts

A	Superscript denoting parameters/variables of the adjustment market.
B	Superscript denoting parameters/variables of the battery system.
bu, se	Superscripts denoting selling or buying actions in the adjustment market.
C	Superscript denoting parameters/variables of the CSP system.
ch, dis	Superscripts denoting the operating status of the battery system, charging or discharging.
D	Superscript denoting parameters/variables of the DA market.
DR	Superscript denoting parameters/variables of the DRP.
FE	Superscript denoting the state of producing power directly by the solar field.

FS	Superscript denoting the state of transfering power from the solar field to thermal storage.
S	Superscript denoting parameters/variables of the thermal storage.
SE	Superscript denoting the state of producing power directly by the thermal storage.
Sys	Superscript denoting parameters/variables of the entire system.
Tot	Superscript denoting the final planned energy.
W	Superscript denoting parameters/variables of wind turbines.

Variables

Profit	Variable indicating the obtained profit, €.
x	Commitment state of the CSP system, 0 or 1.
z	Battery's running state, 0 or 1.
$\epsilon_{\mathrm{s}}, \sigma$	Supplementary variables employed for CVaR computation.
$\varkappa$	Volume of stored electric power, MWh.
Λ^{+}, Λ^{-}	Over- and under-generation energy deviation, MWh.
ξ	Electric offering powers, MW.
ϖ	Load shedding offer, MW.
ς	Thermal power, MW.

Parameters

Ca	Nominal capacity, MW.
EF	Forecasted power profile of the solar field, MW.
L_0	DRP's load prior to the load shedding, MW.
P	Forecasted power profile of wind turbines, MW.
q	Time period duration, h.
$\mathrm{RUR}, \mathrm{RDR}$	Ramp-up and ramp-down bounds of thermal storage, MW/h.
S	Blocks' slope.
α	Confidence level.
$\beta_1, \beta_2, \beta_3$	Conversion efficiencies in various parts of the CSP system.
ε	Battery's efficiency in various running states.
ι^{+}, ι^{-}	Over- and under-generation imbalance price ratio.
$\varkappa^{\mathrm{B,Max}}$	Upper boundary of stored electric energy in the battery, MWh.
λ	Parameter determining the extent of load shedding offers in an hour.
π_s	Probability of scenario s.
ρ	Parameter determining the extent of load shedding offers within the time frame.

ϱ	Market price, €/MWh.
ϱ^*	Rate of incentive payment, €/MWh.
$\varsigma^{\text{S,Max}}, \varsigma^{\text{S,Min}}$	Technical maximum and minimum values of stored energy in thermal storage, MWh.
φ	Constant factor linking load and price.

Other Symbols

F	Objective function.
$\underline{(.)}, \overline{(.)}$	Symbols denoting lower and upper boundaries of parameters/variables.
$(.)^{\text{r}}, (.)^{\text{m}}$	Symbols denoting radius and midpoint of variables.

Abbreviations

CSP	Concentrated Solar Power.
CVaR	Conditional Value-at-Risk.
DA	Day-ahead.
DRP	Demand Response Provider.
HPGC	Hybrid Power Generation Company.
MSI	Mixed Stochastic-Interval.
IGDT	Information Gap Decision Theory.
NBI	Normal boundary intersection.

References

[1] T. A. Deetjen, J. D. Rhodes, and M. E. Webber, "The impacts of wind and solar on grid flexibility requirements in the Electric Reliability Council of Texas," *Energy*, vol. 123, pp. 637–654, 2017.

[2] N. Pearre and L. Swan, "Reimagining renewable electricity grid management with dispatchable generation to stabilize energy storage," *Energy*, p. 117917, 2020.

[3] C. Schoeneberger, C. McMillan, P. Kurup, S. Akar, R. Margolis, and E. Masanet, "Solar for industrial process heat: A review of technologies, analysis approaches, and potential applications in the United States," *Energy*, p. 118083, 2020.

[4] O. Ogunmodimu and E. C. Okoroigwe, "Concentrating solar power technologies for solar thermal grid electricity in Nigeria: A review," *Renew. Sustain. Energy Rev.*, vol. 90, pp. 104–119, 2018.

[5] J. Ji, H. Tang, and P. Jin, "Economic potential to develop concentrating solar power in China: A provincial assessment," *Renew. Sustain. Energy Rev.*, vol. 114, p. 109279, 2019.

[6] E. Du et al., "Operation of a high renewable penetrated power system with CSP plants: a look-ahead stochastic unit commitment model," *IEEE Trans. Power Syst.*, vol. 34, no. 1, pp. 140–151, 2018.

[7] E. Du et al., "The role of concentrating solar power toward high renewable energy penetrated power systems," *IEEE Trans. Power Syst.*, vol. 33, no. 6, pp. 6630–6641, 2018.

[8] T. Xu and N. Zhang, "Coordinated operation of concentrated solar power and wind resources for the provision of energy and reserve services," *IEEE Trans. Power Syst.*, vol. 32, no. 2, pp. 1260–1271, 2016.

[9] R. Dominguez, L. Baringo, and A. J. Conejo, "Optimal offering strategy for a concentrating solar power plant," *Appl. Energy*, vol. 98, pp. 316–325, 2012.

[10] Y. Zhao, Z. Lin, F. Wen, Y. Ding, J. Hou, and L. Yang, "Risk-Constrained Day-Ahead Scheduling for Concentrating Solar Power Plants With Demand Response Using Info-Gap Theory," *IEEE Trans. Ind. Informatics*, vol. 15, no. 10, pp. 5475–5488, 2019.

[11] G. He, Q. Chen, C. Kang, and Q. Xia, "Optimal Offering Strategy for Concentrating Solar Power Plants in Joint Energy, Reserve and Regulation Markets," *IEEE Trans. Sustain. Energy*, vol. 7, no. 3, pp. 1245–1254, 2016.

[12] D. Yu, A. G. Ebadi, K. Jermsittiparsert, N. H. Jabarullah, M. V. Vasiljeva, and S. Nojavan, "Risk-constrained Stochastic Optimization of a Concentrating Solar Power Plant," *IEEE Trans. Sustain. Energy*, 2019.

[13] Z. Wu, M. Zhou, J. Wang, E. Du, N. Zhang, and G. Li, "Profit-Sharing Mechanism for Aggregation of Wind Farms and Concentrating Solar Power," *IEEE Trans. Sustain. Energy*, 2020.

[14] Fang Y, Zhao S. Look-ahead bidding strategy for concentrating solar power plants with wind farms. Energy 2020:117895.

[15] J. Zhao, C. Wan, Z. Xu, and J. Wang, "Risk-based day-ahead scheduling of electric vehicle aggregator using information gap decision theory," *IEEE Trans. Smart Grid*, vol. 8, no. 4, pp. 1609–1618, 2015.

[16] E. Moiseeva and M. R. Hesamzadeh, "Strategic Bidding of a Hydropower Producer under Uncertainty: Modified Benders Approach," *IEEE Trans. Power Syst.*, vol. 8950, no. c, pp. 1–1, 2017.

[17] N. Mazzi, J. Kazempour, and P. Pinson, "Price-taker offering strategy in electricity pay-as-bid markets," *IEEE Trans. Power Syst.*, vol. 33, no. 2, pp. 2175–2183, 2017.

[18] S. Shafiee, H. Zareipour, and A. M. Knight, "Developing bidding and offering curves of a price-maker energy storage facility based on robust optimization," *IEEE Trans. Smart Grid*, vol. 10, no. 1, pp. 650–660, 2017.

[19] I. N. Moghaddam, B. Chowdhury, and M. Doostan, "Optimal sizing and operation of battery energy storage systems connected to wind farms participating in electricity markets," *IEEE Trans. Sustain. Energy*, vol. 10, no. 3, pp. 1184–1193, 2018.

[20] M. K. AlAshery, D. Xiao, and W. Qiao, "Second-Order Stochastic Dominance Constraints for Risk Management of a Wind Power Producer's Optimal Bidding Strategy," *IEEE Trans. Sustain. Energy*, 2019.

[21] K. Pan and Y. Guan, "Data-driven risk-averse stochastic self-scheduling for combined-cycle units," *IEEE Trans. Ind. Informatics*, vol. 13, no. 6, pp. 3058–3069, 2017.

[22] Hasankhani A, Hakimi SM. Stochastic energy management of smart microgrid with intermittent renewable energy resources in electricity market. Energy 2021;219:119668.

[23] Koltsaklis NE, Giannakakis M, Georgiadis MC. Optimal energy planning and scheduling of microgrids. Chem Eng Res Des 2018;131:318–32.

[24] Fazlalipour P, Ehsan M, Mohammadi-Ivatloo B. Risk-aware stochastic bidding strategy of renewable micro-grids in day-ahead and real-time markets. Energy 2019;171:689–700.

[25] Çavuş Ö, Kocaman AS, Yılmaz Ö. A risk-averse approach for the planning of a hybrid energy system with conventional hydropower. Comput Oper Res 2021;126:105092.

[26] Khaloie H, Anvari-Moghaddam A. Robust Optimization Approach for Generation Scheduling of a Hybrid Thermal-Energy Storage System. 2020 IEEE 29th Int. Symp. Ind. Electron., IEEE; 2020, p. 971–6.

[27] Khaloie H, Abdollahi A, Rashidinejad M, Siano P. Risk-based probabilistic-possibilistic self-scheduling considering high-impact low-probability events uncertainty. Int J Electr Power Energy Syst 2019;110:598–612. https://doi.org/10.1016/j.ijepes.2019.03.021.

[28] Xu X, Hu W, Cao D, Huang Q, Liu Z, Liu W, et al. Scheduling of wind-battery hybrid system in the electricity market using distributionally robust optimization. Renew Energy 2020;156:47–56.

[29] Faraji J, Ketabi A, Hashemi-Dezaki H, Shafie-Khah M, Catalão JPS. Optimal day-ahead self-scheduling and operation of prosumer microgrids using hybrid machine learning-based weather and load forecasting. IEEE Access 2020;8:157284–305.

[30] Faraji J, Ketabi A, Hashemi-Dezaki H, Shafie-Khah M, Catalao JPS. Optimal day-ahead scheduling and operation of the prosumer by considering

corrective actions based on very short-term load forecasting. IEEE Access 2020;8:83561–82.

[31] Y. Jiang, C. Wan, C. Chen, M. Shahidehpour, and Y. Song, "A hybrid stochastic-interval operation strategy for multi-energy microgrids," *IEEE Trans. Smart Grid*, vol. 11, no. 1, pp. 440–456, 2019.

[32] H. Khaloie et al., "Coordinated wind-thermal-energy storage offering strategy in energy and spinning reserve markets using a multi-stage model," *Appl. Energy*, vol. 259, p. 114168, Feb. 2020.

[33] L. Bai, F. Li, H. Cui, T. Jiang, H. Sun, and J. Zhu, "Interval optimization based operating strategy for gas-electricity integrated energy systems considering demand response and wind uncertainty," *Appl. Energy*, vol. 167, pp. 270–279, 2016.

[34] H. Khaloie, M. Mollahassani-pour, and A. Anvari-Moghaddam, "Optimal Behavior of a Hybrid Power Producer in Day-Ahead and Intraday Markets: A Bi-Objective CVaR-Based Approach," *IEEE Trans. Sustain. Energy*, p. 1, 2020.

[35] Khaloie H, Abdollahi A, Nojavan S, Shafie-Khah M, Anvari-Moghaddam A, Siano P, et al. Offering Strategy of Thermal-Photovoltaic-Storage Based Generation Company in Day-Ahead Market. Electr. Mark., Springer; 2020, p. 113–33.

[36] Khaloie H, Abdollahi A, Shafie-Khah M, Siano P, Nojavan S, Anvari-Moghaddam A, et al. Co-optimized bidding strategy of an integrated wind-thermal-photovoltaic system in deregulated electricity market under uncertainties. J Clean Prod 2020;242:118434. https://doi.org/10.1016/j.jclepro.2019.118434.

[37] Hasankhani A, Hakimi SM, Shafie-khah M, Asadolahi H. Blockchain technology in the future smart grids: A comprehensive review and frameworks. Int J Electr Power Energy Syst 2021;129:106811.

[38] J. Liang and W. Tang, "Interval based transmission contingency-constrained unit commitment for integrated energy systems with high renewable penetration," *Int. J. Electr. Power Energy Syst.*, vol. 119, p. 105853, 2020.

[39] J. Aghaei, M. A. Akbari, A. Roosta, and A. Baharvandi, "Multiobjective generation expansion planning considering power system adequacy," *Electr. power Syst. Res.*, vol. 102, pp. 8–19, 2013.

[40] Khaloie H, Anvari-Moghaddam A, Hatziargyriou N, Contreras J. Risk-constrained self-scheduling of a hybrid power plant considering interval-based intraday demand response exchange market prices. J Clean Prod 2021;282:125344. https://doi.org/https://doi.org/10.1016/j.jclepro.2020.125344.

[41] "Weather history+ - meteoblue." [Online]. Available: https://www.meteoblue.com/en/historyplus. [Accessed: 22-Apr-2019].

[42] "Bienvenido — ESIOS electricidad · datos · transparencia." [Online]. Available: https://www.esios.ree.es/es. [Accessed: 14-Mar-2019].